

Functional High-Definition 3D Studies of the Lumbar Spine Using Magnetic Resonance Imaging

K. E. W. Eberhardt¹, B. F. Tomandl¹, C. Rezk-Salama², R. Schindler³, W. Huk¹, M. Lell⁴

¹Div. of Neuroradiology, Dept. of Neurosurgery, University of Erlangen-Nuremberg, Erlangen, Germany

²Institute for Graphic Data Processing, University of Erlangen-Nuremberg, Erlangen, Germany

³Inside, Funktionelle Diagnostik GmbH (Functional Diagnostic Technology, Inc.), Schweinfurt, Germany

⁴Institute for Diagnostic Radiology, University of Erlangen-Nuremberg, Erlangen, Germany

Keywords

• MRI • myelography • skeletal axial • spine
• computer application 3D

Introduction

Functional in vivo studies of the lumbar spine using open MRI systems are described in literature [1-4]. So far only 2D sequences with low spatial resolution have been used due to the low field strength of these systems as well as their coil design. Additionally, 3D measurements, the prerequisite for precise volumetry, have been described only for cadaver studies [3, 5]. With this type of study, measurements were performed in both flexion and extension while determining the width of the spinal canal. Functionally-related changes in the spinal nerve foramen have been described in two studies only. However, in these, the functional measurements from an open MRI System (0.5T) were compared to standard results from a bore-type MRI system (1.0T) [4, 6]. To date, a comprehensive display of complex changes in the locomotor system of the lumbar spine and their effects on CSF space and relevant nerve roots has not been possible. The objective of the present study was to find and optimize suitable sequences on a high-field system (1.5T) using a flexible coil system. These sequences were used to display osteoligamentary structures as well as the nerve roots and the CSF space. Additionally, it would be possible to measure changes in the respective functional status. The volumetry of the CSF space is suitable for monitoring progress following therapy for herniated disks.

Material and Method

Measurements were performed using commercial 1.5 Tesla whole-body system (MAGNETOM Symphony, Siemens AG, Medical Solutions, Erlangen). For signal improvement, a combination of surface coils was used. The following sequences were applied:

FLASH in-opposed phase is a gradient echo sequence with bipolar read-out gradients [7] originally developed for liver diagnostics (Fig. 1). The TR of the sequence is 121.4 ms, the echo time ($TE_{1/2}$) 2.4/4.8 ms and the excitation angle $\alpha = 70^\circ$. The total acquisition time is 35 s with a slice thickness of 5 mm, an FoV of 320 mm and a 256 x 256 matrix. The bone matrix as well as the nucleus pulposus are shown in the opposed phase; the outline of bone in the in-phase, with the highest contrast. For this reason, this sequence was used to measure mobility using sagittal images for flexion and extension.

MEDIC-3D is also a gradient echo sequence (Fig. 2). As compared to conventional T_2^* sequences which are susceptible to magnetic field inhomogeneities due to their low readout gradients, the MEDIC 3D sequence is characterized by multiple, unipolar, high readout gradients. The TR is 60 ms, the TE is 4 ms, and the excitation angle is $\alpha = 9^\circ$. Our measurements used a slice thickness of 1.17 mm, a FoV of 250 mm, and a 256 x 256 matrix. The total measurement time was 6.5 min. This sequence was used to image the CSF space.

The test persons were positioned on a pneumatic positioning support (Inside, Functional Diagnostics Technology, Schweinfurt). The support could be adjusted to their individual size allowing for a constant, reproducible kyphosis and lordosis position (Fig. 3) during the examination. Several combinable surface coils integrated into the positioning support provided the necessary signal-to-noise ratio.

Test Persons and Their Data

A total of 24 females and 19 males were examined. The average age of the test persons was 38.02 years (standard deviation: 8.98 years). The average height was 173.60 cm (standard deviation: 9.67 cm), and the average weight was 71.45 kg (standard deviation: 16.62 kg).

Measurements

One FLASH in-opposed phase and one MEDIC 3D sequence each were performed in normal position,

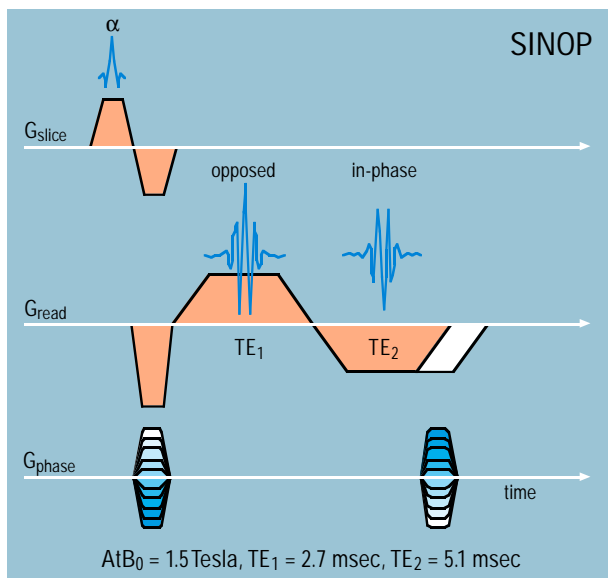


Fig. 1
FLASH in-opposed phase sequence diagram: Gradient echo sequence with bipolar readout gradients. The magnetization of fat and water protons is antiparallel at TE₁ (opposed-phase) and parallel at TE₂ (in-phase).
The contrast changes according to the amount of fat and water in a voxel (tissue parameter). The signal characteristics may be changed by varying TR, TE and α (sequence parameters).

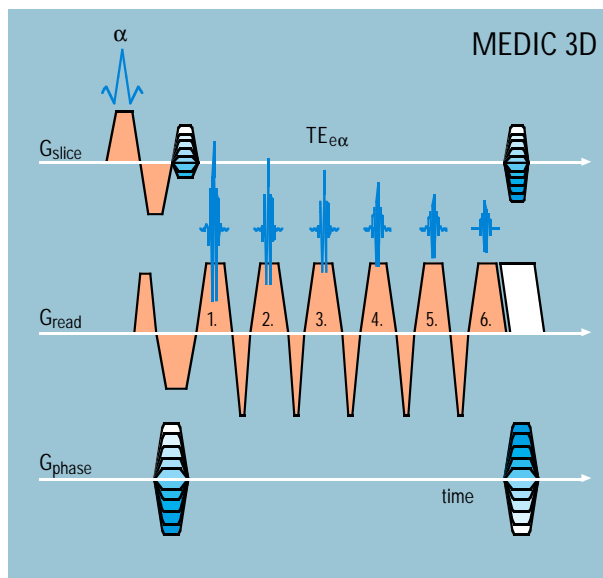


Fig. 2
MEDIC 3D sequence diagram. Gradient echo sequence with unipolar, multiple readout gradients with high amplitude. Significantly reduced flow sensitivity through GMR.
T₂*-weighting by adding the individual echo data. The signal characteristics are comparable to those in a FLASH sequence.

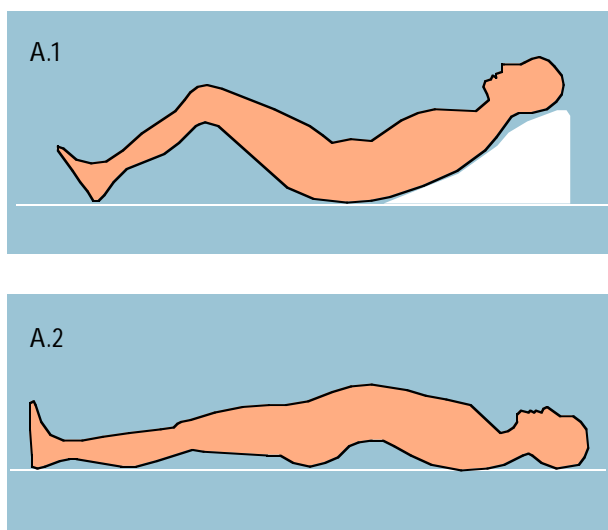


Fig. 3
Patient positioning using special positioning support (shaded).
A.1: Flexion position,
A.2: Extension position.

flexion and extension. Measurements were performed in sagittal slice orientation with a cranio-caudal phase-encoding direction. The slice thickness in this case was 1.2 mm. A body array coil was added to the spine array coil during extension to compensate for the signal loss caused by changes in the coil/object distance.

Post-Processing

Segmentation and 3D visualization were performed at an SGI Onyx 2 workstation (R 10000, 195 MHz, Base Reality Graphics, 64 MB 3D texture memory).

Segmentation

Due to the signal characteristics of the MEDIC 3D sequence, implicit segmentation via a transfer function across the entire volume proved to be difficult. Fluid, disk, veins and ligaments, all showed high signal intensity. For this reason, a semi-automatic explicit segmentation was applied [8].

Onyx is a trademark of Silicon Graphics, Inc.

Visualization

For visualization, direct volume rendering using 3D texture mapping was used [8-9]. Pre-defined color tables were used to accelerate and standardize this method of visualization.

Volumetry

A segmented MEDIC 3D data set provides a conventional display of the CSF space similar to conventional myelography. However, unlike conventional myelography, the image is shown in 3D display, allowing for exact volume measurements. For the purpose of standardization, the volume to be measured was established using a reference point as the basis. It was set at 5 mm in cranial and at 5 mm in caudal direction. The reference point used was the center of the respective intervertebral space. This measurement point remained parallel to the intervertebral space. To determine the volume of the periradicular fluid spaces, the so-called axilla was established as a reference point by applying a tangent to the dural sac (in the vicinity of the nerve roots exiting from the dural sac). The length of the measurement box was such as to extend from the axilla section to the spinal ganglion, and the tilt of the box was adjusted to the course of the spinal nerves.

Measurement of the Range of Motion and Volumetry of the CSF Space

The data from the FLASH in-opposed phase sequence were used for the measurements, since they allow for exact delineation of the bones to their surroundings. To determine segmental mobility, the angle between the upper plate of the lower vertebra to the back edge of the higher vertebra was measured for all segments from L1-S1, as proposed by Dupuis [10]. The angular differences in the functional positions indicated the range of motion.

Subsequently, the associated fluid volumes (spinal as well as periradicular) were determined in the respective segments. To obtain a comparison independent of the absolute volume, the difference in volume between flexion and extension was normalized to the flexion volume. $((Vol F - Vol E) / Vol F)$. These normalized volume differences were then correlated to the angular differences.

Statistics

Mean value and standard deviation were determined for all angle and volume measurements (SPSS 9, SPSS Software, Munich, Germany). The statistical analysis was based on a significance level of $\alpha = 0.05$. The connection between changes in angle and volume were computed using correlation analysis (Pearson's correlation coefficient).

Results

For functional measurements, the limited spatial conditions in the gantry of a bore-type high-field MR

tomograph necessitate off-center measurements. However, the MAP shim implemented in the sequence protocol was sufficient for optimizing the homogeneity in the measurement volume to an extent that eliminated artifacts as well as related signal loss. A sufficient signal-to-noise ratio was obtained by using a combination of spine and body-array coils. Motion artifacts, caused in particular by abdominal breathing during extension, were greatly reduced by a cranio-caudal phase-encoding direction.

The MEDIC 3D sequence showed high signal for the vertebral disks, ligaments and joint surfaces. However, they can clearly delineated from the strongly hyperintense fluid space including nerve root sheaths containing fluid. In all volunteers, the sequence allows for a well-defined exit of the spinal nerves, the so-called axilla up to the spinal ganglion, without reduced signal. Within the hyperintense fluid, the root nerves were displayed as hypointense structures (Table 1). In contrast to other T₂-weighted sequences such as a turbo spin-echo or CISS sequence, the MEDIC 3D sequence displays cerebrospinal signals extending to the spinal ganglion (Fig. 4).

The images of the MEDIC 3D sequence convert into a three-dimensional image of the CSF space (3D myelography) through post-processing via volume rendering. Analogous to conventional X-ray myelography, the spinal nerves are shown within the CSF space as low-signal structures. Using region growing technique, bones may be displayed from the same measurement data (Fig. 5).

Evaluation	MEDIC 3D	
	n	%
CSF space		
Axilla smooth boundaries	20	100
Root nerve symmetr.	20	100
Ganglion visualized	20	100
Spinal nerves		
Intradural portion visible		
1.17 mm	18	90
2.00 mm	10	50
Ligaments		
Signal-emitting definable	20	100
Disk tissue		
Signal-emitting definable	20	100
Bones		
Sufficiently definable	20	100

Table 1
Visualization results after post-processing with volume rendering.

In addition, other segmented subvolumes such as arterial and venous vessels may be included in the overall visualization (Fig. 6).

Angle Measurement and Volumetry

While the outlines of disks are shown with high contrast when in phase, the opposed phase of the FLASH

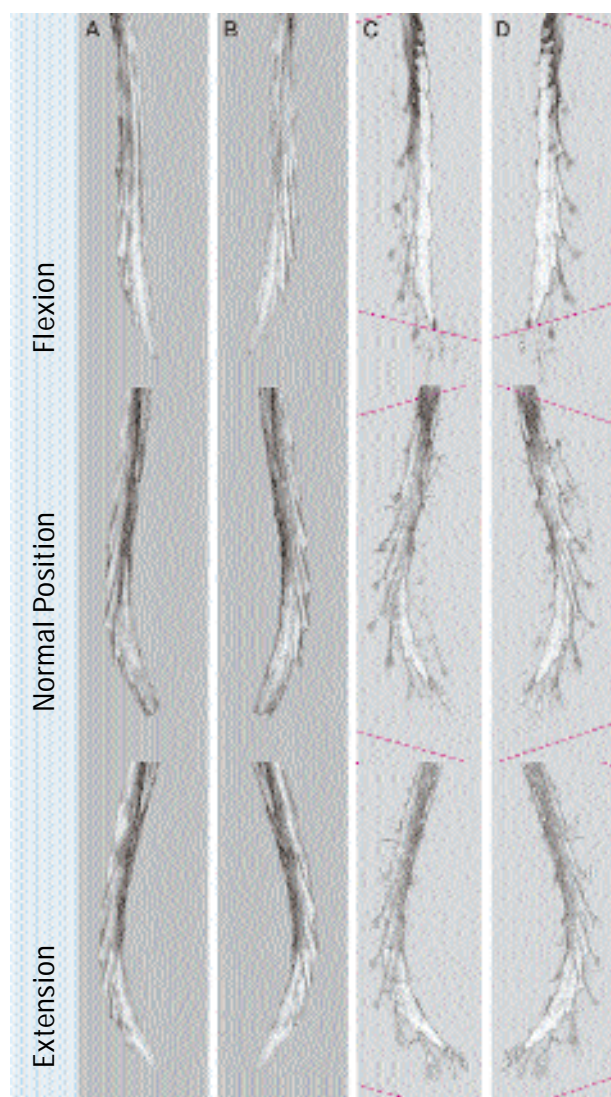


Fig. 4
The set of images on the left shows the images of a CISS 3D data set. A MEDIC 3D data set is shown in the set of images on the right.

As compared to the MEDIC 3D data set, the peripheral spinal nerves are not visualized in the CISS 3D data set.

A-B: CISS 3D sequence,
C-D: MEDIC 3D sequence.

in-opposed phase sequence is suitable for displaying the bone matrix and the nucleus pulposus. For this reason, in-phase images are used to determine the angular difference between flexion and extension according to the Dupuis method [10]. The results are presented in Table 2. The mean values for the range of motion for our measurements were between 13.0° (L1-2) and 16.7° (L5-S1).

The functional changes of the respective position on the CSF space were determined with the MEDIC 3D sequence. The difference in volumes in flexion/extension from the volume in the normal position was determined for each moving segment (Table 2).

In the flexion position, the segmental volume of the CSF increased between 5.3% (L2-3) and 9.6% (L4-5); in the extension position it increased between 9.2% (L1-2) and 21.5% (L5-S1) in comparison to the normal volume.

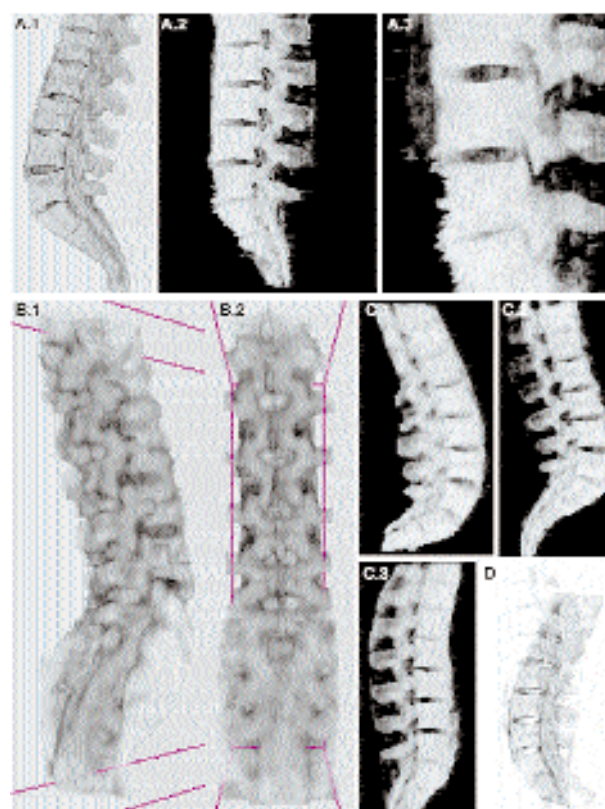


Fig. 5
A.1: The medial clip plane shows the spinal canal in normal position.
A.2: Lateral clip plane with visualization of the foramina during flexion.
A.3: Detailed view of the facets.
B.1 and B.2: Dorsal and dorso-lateral view of the lumbar spine and the sacrum.

C.1-C.3: Medial clip plane in functional positions. In B and C noise suppression was obtained using anisotropic filtering.
D: Overlapping of flexion and extension.

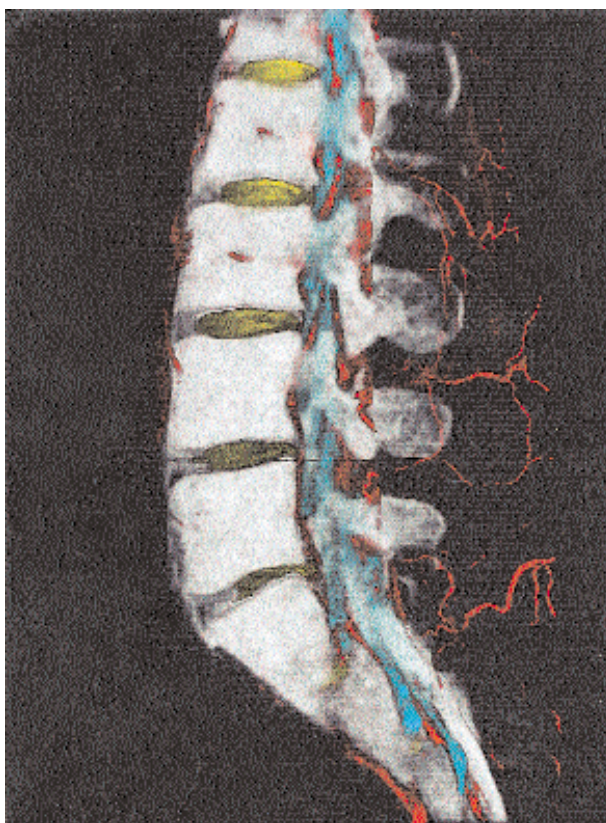


Fig. 6
Three-dimensional visualization
of a 3D data set (MEDIC 3D).

Segment	Volunteers ¹		Volunteers ²	
	MV	STDEV	MV	STDEV
L 1/2	13.0	2.01	11.9	No information
L 2/3	13.7	2.77	14.5	No information
L 3/4	13.9	2.69	15.3	No information
L 4/5	15.4	3.12	18.2	No information
L 5/S 1	16.7	2.98	17.0	No information

¹Eberhardt ²Dvorak (11)

Table 2
Functional range of motion
of the lumbar spine (angular
difference between flexion and
extension) in 43 volunteers¹.

Fig. 7 shows an analysis of the correlation between the segmental range of motion and the intraspinal and periradicular changes in volume during a functional study of the lumbar spine. Correlations prove the quantitative link between function and cerebrospinal fluid volume: the volume of the cerebrospinal fluid increases in the flexion position and decreases in the extension position. The changes in volume in the moving segment are dependent on the angular difference, i. e., the range of motion.

Discussion

To date, functional measurements of the lumbar spine have been performed in so-called open MRI systems, usually with low field strengths between 0.2 and 0.5T. As a result, the obtainable spatial resolution was insufficient for a high-resolution 3D display of the anatomic structures involved [12, 13]. Our examinations were performed in a bore-type high-field 1.5T system. Patients in the extension position had to be examined outside the magnet isocenter. Our results show that it is possible to perform off-center measurements without related signal loss. During flexion or normal position, the spine array coil will suffice. However, to obtain sufficient signal in the extension position, the body array coil has to be added due to the larger distance between coil and measurement volume. Cranio-caudal phase-encoding proved suitable for reducing motion artifacts. Otherwise, increased abdominal breathing during extension will lead to distinct artifacts.

The range of motion stated in literature [11, 14], measured with patients in the lateral position, corresponds to our measurements in the supine position. Examinations in seated position, possible only with special open magnets at low field strength, allow a slightly larger range of motion [12].

Although the range of motion is very good with open, vertically aligned magnets, resolution is too low to allow for detailed analysis or 3D examinations [12]. Additionally, examinations in the seated position or with the patient in the lateral position are not easily reproducible without patient stabilization [13]. Although the 2D parameters measured in this study (cross-section, distances and surfaces of the spinal canal) show a clear dependence on the respective functional position [15-20], 2D measurement values vary greatly and are difficult to reproduce [13]. A solution to this problem was the use of strong T₂-weighted 3D sequences for "MR myelography". In one of our publications, we were able to show the basic value of this method [15]. A FISP sequence was used. However, it proved to be susceptible to magnet inhomogeneities. Spatial resolution in the Z axis was limited to 1.6 mm at a relatively long measurement time exceeding 7 minutes. Post-processing, performed via implicit segmentation and visualization through MIP resulted in overlapping structures. Since these risk false

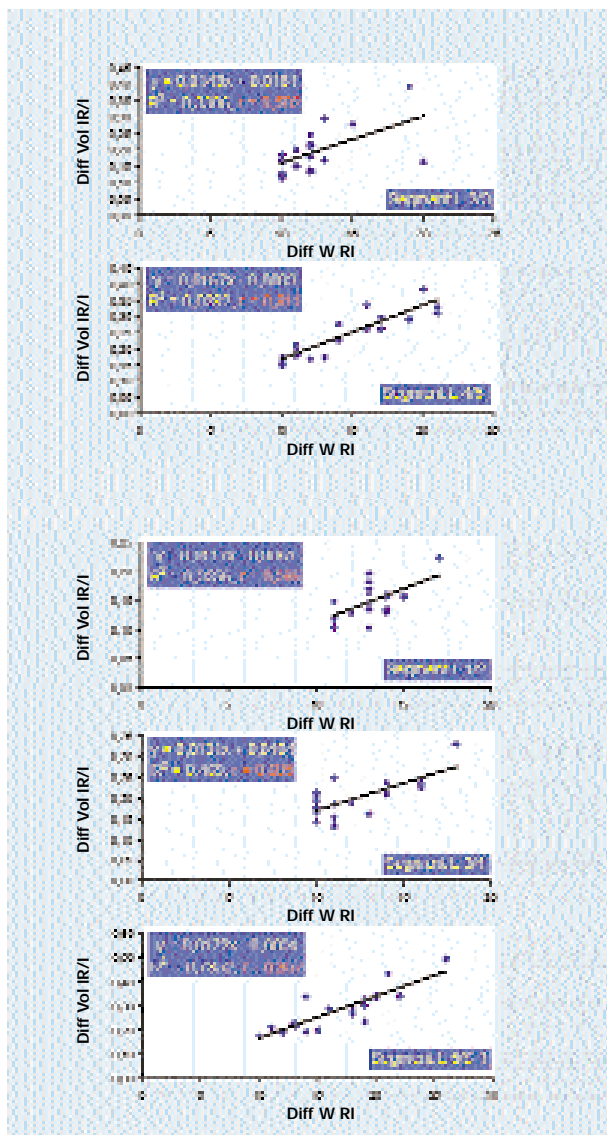


Fig. 7
Correlation between segmental functional range of motion of the lumbar spine and segmental volumes in 20 healthy, young volunteers.

positive findings (overlapping due to structures with high signals such as disks, ligaments and vessels), clinical acceptance of this method was limited [16].

Higher spatial resolution and a better signal-to-noise ratio is possible by using a new MEDIC-3D sequence. This sequence has a higher bandwidth and multiple, high amplitude, unipolar readout gradients that greatly reduces inhomogeneity artifacts in gradient echo sequences. Additionally, the sequence provides for higher spatial resolution at a good signal-to-noise ratio as compared to the FISP sequence used. Both the FISP 3D and the MEDIC 3D are flow-compensated, steady-state sequences [17]. The MEDIC 3D sequence used by us is particularly well suited for post-processing due to its specific signal characteristics (differentiation of the bone matrix from the high-signal, surrounding structures). However, this requires prior explicit, semi-automatic segmentation through region growing. As described in the material and method section, our data were not implicitly segmented (i. e., via a fixed, pre-selected threshold value) but rather explicitly segmented [8-9]. The resulting sub-volumes could then be quantified to give values that are easily reproduced as shown by the validation via phantom measurements. In this manner, quantitative examinations are possible.

In our study, visualization was obtained by means of volume rendering, a technique available since the early 1990s. A current, detailed description of the technique and its application is included in the study by Calhoun et al. [21]. As the visualization results of MR myelograms of the volunteers have shown, the foramina of the spinal nerves from the dural sac, the so-called “axilla” of the peripheral spinal nerves, were well defined in all volunteers, without voids in the surrounding cerebrospinal fluid. Additionally, the peripheral cerebrospinal fluid foramina were visible in all participants, and thus indirectly the spinal nerves up to the spinal ganglion, i. e., the branching of the spinal nerves into the Rami ant. et post., as well as the communicants. The changes of the CSF signals were converted into three-dimensional visualizations, i. e., 3D MR myelography, by means of direct volume rendering.

Our method of quantitative functional MR myelography is therefore a standardized and reliable technique for evaluating compression including that of peripheral spinal nerves. To date, no comparable studies have been published. Of interest are the relatively minimal changes in volume of the intraspinal fluid as compared to the considerable decrease in periradicular fluid volume. In this context, extension from a functional point of view is considerably more important than flexion. There are only two studies that discuss function-related changes in peripheral nerves (signal changes [6] as well as determine the changes in the diameter of the neuroforamen [4]). However, neither 3D visualization nor volumetry was performed. To date, only in vitro volumetries of the

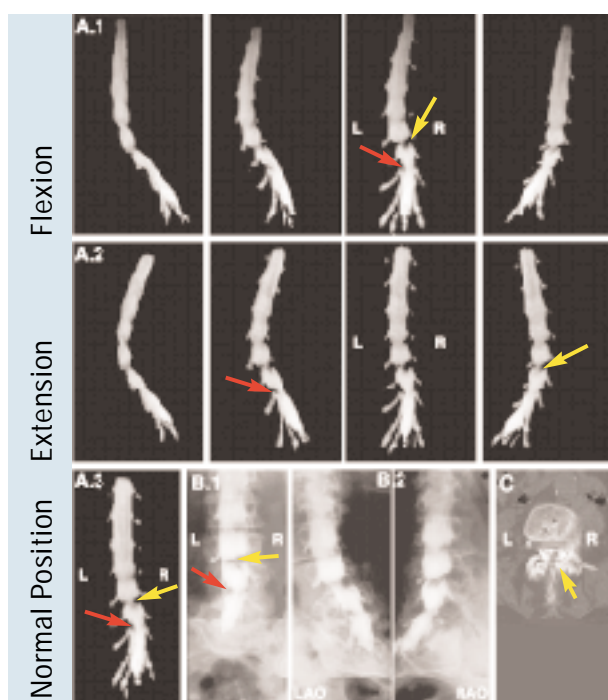


Fig. 8
The functional MR myelography (A.1-3) and the conventional myelography (B.1-2) show a function-related identical high grade filling defect accentuated on the right in segment L3-4 (yellow arrows), and an axillary

contrast medium void on the left side in L4-5 (red arrows).

The post-myelographic CT (C) shows hypertrophied vertebral joints and calcium deposits and thickening of the ligamenta flava as the cause of the stenosis in segment L3-4 (yellow arrow).

dural sac have been described [5]. In agreement with the literature, our functional volume measurements showed an increase in volume during flexion as well as a decrease during extension. The changes in volume correlated with the range of motion in the volunteers. Since comparable functional measurements of the cerebrospinal fluid volume have been performed only by our team, measurement values determined by other groups for 2D measurements are not comparable to our measurements. The correlation we found between the segmental range of motion of the lumbar spine and the changes in the corresponding normalized volume confirms the dependency of the cerebrospinal fluid volume on the functional position, and provides an opportunity for quantifiable functional studies considered especially useful for determining degenerative spinal stenosis.

Summary and Outlook

Our study shows that a sufficient range of motion for functional studies in a bore-type MRI system may be realized by using special positioning equipment. Adequate

spatial resolution for analyzing individual anatomical components may be obtained by using surface coils as well as suitable sequences together with a high field system.

This is necessary for both indication as well as planning of surgical invasions regarding multi-segmented spinal stenoses to determine the height as well as length of the main stenoses so as to delimit the scope of surgery. A secondary spondylolisthesis may be evaluated as well during the functional examination. A clinical example of a 75 year-old patient with bilateral radicular symptoms L3/4 is shown in Fig. 8.

Literature

- [1] Zamani AA, Moriaty T, Hsu L, Winalski CS, Schaffer JL, Isbister H, Schenck JF, Rohling KW, Jolesz F. Functional MRI of the lumbar spine in erect position in a superconducting open-configuration MR system: preliminary results. *J. Magn. Reson. Imaging* 1998; 8(6): 1329-1333.
- [2] Wildermuth S, Zanetti M, Duewll S, Schmid MR, Romanowsky B, Benini A, Boni T, Hodler J. Lumbar spine: quantitative and qualitative assessment of positional (upright flexion and extension) MR imaging and myelography. *Radiology* 1998; 207(2): 391-398.
- [3] Fennell AJ, Jones AP, Huskins DW. Migration of the nucleus pulposus within the intervertebral disc during flexion and extension of the spine. *Spine* 1996; 21(239): 2753-2757.
- [4] Schmid MR, Stucki G, Duewll S, Wildermuth S, Romanowsky B, Hodler J. Changes in cross-sectional measurements of the spinal canal and intervertebral foramina as a function of a position: in vivo studies on an open-configuration MR system. *A.J.R., Am J Roentgenol.* 1999; 172(4): 1095-1102.
- [5] Dai LY, Xu YK, Zhang WM, Zhou ZH. The effect of flexion-extension motion of the lumbar spine on the capacity of the spinal canal. An experimental study. *Spine* 1989; 14(5): 523-525.

[6] Weishaupt D, Schmid MR, Zanetti M, Boos N, Romanowski B, Kissling RO, Dvorak J, Hodler J. Positional MR imaging of the lumbar spine: does it demonstrate nerve root compromise not visible at conventional MR imaging? *Radiology* 2000; 215(1): 247-253.

[7] Taupitz M, Deimling M, Malcher R, Schröter T, Bollow M, Hamm B. A new rapid T₁-weighted multiplanar spoiled gradient-echo sequence for simultaneous acquisition of in-phase and opposed-phase images (SINOP). Proceedings of the 6th International Society of Magnetic Resonance in Medicine (ISMRM), Sydney, Australia 1998: 517.

[8] Rezk-Salama C, Hastreiter P, Eberhardt KEW, Tomandl BF, Ertl T. Interactive direct volume rendering of dural arteriovenous fistulae. In: Proceedings. MICCAI 1998: 42-51.

[9] Engel K, Hastreiter P, Tomandl BF, Eberhardt KEW, Ertl T. Combining local and remote visualization techniques for interactive volume rendering in medical applications. Accepted for publication in Proceedings Visualization '2000, IEEE, Salt Lake City, US, 2000.

[10] Dupuis PR, Yong-Hing K, Cassidy JD, Kirkaldy-Willis WH. Radiologic diagnosis of degenerative lumbar spinal instability. *Spine* 1985; 10: 262-276.

[11] Dvorak J, Panjabi M, et al. Functional radiographic diagnosis of the lumbar spine. *Spine* 1991; 16: 562-571.

[12] Vitzthum HE, König A, Seifert V. Dynamic examination of the lumbar spine by using vertical, open magnetic resonance imaging. *J. Neurosurg. (Spine1)* 2000; 93: 58-64.

[13] Smith BM, Hurwitz EL, Solsberg D, Rubinstein D, Corenman DS, Dwyer AP, Kleiner J. Interobserver reliability of detecting lumbar intervertebral disc high-intensity zone on magnetic resonance imaging and association of high-intensity zone with pain and anular disruption. *Spine* 1998; 23(19): 2074-80.

[14] Percy M, Portek I, Shepherd J. Three-dimensional x-ray analysis of normal movement in the lumbar spine. *Spine* 1984; 9(3): 294-297.

[15] Eberhardt KEW, Hollenbach HP, Huk WJ. 3D-MR-Myelography (3D-MRM) of the lumbar spine. Comparative case study to conventional x-ray myelography. *Eur Radiol*, 1996; 7(5): 737-742.

[16] Thornton MJ, Lee MJ, Pender S, McGrath FP, Brennan RP, Varghese JC. Evaluation of the role of magnetic resonance myelography in lumbar spine imaging. *Eur Radiol* 1999; 9(5): 924-929.

[17] Gyngell ML. Application of the steady-state free precession in rapid 2-DFT NMR imaging: Fast and CE-fast sequences. *Magn. Reson. Imaging* 1988; 6: 415-419.

[18] Wildermuth S, Zanetti M, Duewelle S, Schmid MR, Romanowsky B, Benini A, Boni T, Hodler J. Lumbar spine: quantitative and qualitative assessment of positional (upright flexion and extension) MR imaging and myelography. *Radiology* 1998; 207(2): 391-398.

[19] Fennell AJ, Jones AP, Huskins DW. Migration of the nucleus pulposus within the intervertebral disc during flexion and extension of the spine. *Spine* 1996; 21(239): 2753-2757.

[20] Schmid MR, Stucki G, Duewelle S, Wildermuth S, Romanowsky B, Hodler J. Changes in cross-sectional measurements of the spinal canal and intervertebral foramina as a function of a position: in vivo studies on an open-configuration MR system. *A.J.R., Am J Roentgenol*. 1999; 172(4): 1095-1102.

[21] Calhoun PS, Kuszyk BS, Heath DG, Carley CC, Fishman EK. Three-dimensional Volume rendering of spiral CT data: Theory and Method. *RadioGraphics* 1999; 19: 745-764.

Abbreviations

CISS	= Constructive Interference Steady State
CT	= Computed Tomography
FISP	= Fast Imaging with Steady State Precession
FLASH	= Fast Low Angle Shot
FoV	= Field of View
GMR	= Gradient Motion Rephasing (flow compensation)
MAP	= Multi Angle Projection
MEDIC-3D	= Multi Echo Data Image Combination
MIP	= Maximum Intensity Projection
MRI	= Magnetic Resonance Imaging
TE	= Echo Time
TR	= Repetition Time
VR	= Volume Rendering

Author's address

Dr. K. E. W. Eberhardt
Abteilung für Neuroradiologie
Neurochirurgische Universitätsklinik, Erlangen-Nürnberg
Schwabachanlage 6
D-91054 Erlangen,
Germany

Tel.: +49-(0)9131-8539388
Fax: +49-(0)9131-8536172
e-Mail: keweberhardt@hotmail.com